EFFECT OF RADIATION ON SHOCK STRUCTURE WHEN TEMPERATURE IS NOT VERY HIGH

PHOOLAN PRASAD

Indian Institute of Science, Bangalore

(*Received* 4 *July* 1968)

An approximate analytical solution, which gives the distribution of flow variables in terms of optical thickness from the embedded shock when $\bar{P} < \bar{P}^*$ has been obtained. The jump in the flow variables across the embedded shock has also been obtained. Numerical results are given for six sets of values of M and $\bar{P}$.

Recently a great deal of attention has been focussed on the problem of determining shock-structure in Radiaton-Gas-Dynamics (RGD) based on the continuum equations of gas dynamics, including energy transport by radiation and neglecting viscosity and heat-conduction. In a previous paper[1] we have discussed steady state flows in RGD when radiation pressure is negligible compared with the gas pressure and we have shown that the flow through the shock structure is just one particular steady flow which joins two uniform states, one at $x = +\infty$ and another at $x = -\infty$. We have also discussed the results of Zel'dovich[2] and Heaslet & Baldwin[3] on shock structure with a few new results. The steady state flows in RGD can be studied with the help of a first order ordinary differential equation in particle velocity and radiation pressure with two independent parameters M and $\bar{P}$. For the shock structure, M represents the ratio of the shock speed to the sound velocity in the front of the stationary shock at $x = +\infty$. The second parameter $\bar{P}$ depends only on the thermodynamic state of the fluid at $x = +\infty$. $\bar{P}$ is monotonically increasing function of temperature but monotonically decreasing function of the mass density. When $\bar{P}$ is less than a certain critical value ($\bar{P}^*$), depending on M, a continuous flow through shock structure is not possible, i.e. an embedded shock appears and particle velocity, gas pressure, temperature and mass density are discontinuous across it, whereas radiation flux and radiation energy density are continuous across it. Again if the shock is sufficiently strong, i.e. the shock strength M is greater than a certain critical value (M^*) a continuous flow through the shock is not possible and an embedded shock appears in the flow. In any case, the variation of flow variables through the shock structure is obtained by numerical integration of the differential equations.

In this paper, we have obtained very simple expressions for flow variables in terms of the optical thickness from the shock in the case $\bar{P} < \bar{P}^*$, by approximating the integral curves by straight lines on the two sides of the shock. We mention here that a similar approximate solution is also given by Heaslet & Baldwin[3] and Lick[4] and Vincenti & Kruger[5]. In physical situations, which we come across most frequently, we find that $\bar{P} < \bar{P}^*$ and hence we feel that it is worth obtaining the solution presented here from our phase plane analysis of steady state flows[1] and present some numerical results.

BASIC EQUATIONS

In the frame of reference moving with the shock in an infinite medium, the motion is steady and the one-dimensional equations of mass, momentum and energy give us

$$\rho u = m\,, \tag{1}$$

$$mu + p_G = mc_1 \tag{2}$$

and

$$\frac{p_G}{(\gamma-1)\rho} + \frac{1}{2}u^2 + \frac{u}{m}p_G + \frac{F}{m} = mc_2 \tag{3}$$

where u is particle velocity, ρ mass density, p_G gas pressure, F radiation flux in positive x-direction and m, c_1, c_2 are constants.

As shown by Prasad[1], under Milne-Eddington approximation, the radiative transfer equation and the expression for the radiation pressure give us

$$\frac{dF}{d\tau} = 4\sigma T^4 - 3cp_R \tag{4}$$

and

$$c\frac{dp_R}{d\tau} + F = 0 \tag{5}$$

where c is the velocity of light, p_R radiation pressure, T temperature, σ Stefan constant and τ the optical thickness measured from the shock. Denoting the flow variables in the uniform state at $x = +\infty$ by suffix 1, we introduce the following non-dimensional quantities :

$$\left.\begin{aligned}
&\bar{u} = \frac{u}{u_1}\,, \quad \bar{p}_G = \frac{p_G}{\rho_1 u_1^2}\,, \quad \bar{h} = -\frac{cp_R}{\rho_1 u_1^3}\,,\\
&\bar{\rho} = \frac{\rho}{\rho_1}\,, \quad \bar{F} = \frac{F}{\rho_1 u_1^3}\,, \quad M = -\frac{u_1}{a_{s1}}\,,\\
&Q = 1 + \frac{1}{\gamma M^2}\,, \quad \bar{P} = \frac{\sigma(\gamma T_1)^{5/2}}{\rho_1 R^{3/2}}
\end{aligned}\right\} \tag{6}$$

where $a_s^2 = \dfrac{\gamma p_G}{\rho}$, $u_1 < 0$, R is the gas constant appearing in the equation of state :

$$p_G = R\rho T \tag{7}$$

and γ is the ratio of specific heats.

From the above equations we can easily derive

$$\bar{p}_G = Q - \bar{u} \tag{8}$$

$$\frac{d\bar{h}}{d\tau} = \bar{F} = -\frac{\gamma+1}{2(\gamma-1)}(1-\bar{u})(\bar{u}-\bar{u}_2) \tag{9}$$

$$\frac{d\bar{F}}{d\tau} = 3\left[\bar{h} - \frac{4}{3}\bar{P}M^5\left\{\bar{u}(Q-\bar{u})\right\}^4\right] \tag{10}$$

and

$$\frac{d\bar{u}}{d\bar{h}} = -6\left(\frac{\gamma-1}{\gamma+1}\right)^2 \frac{\bar{h} - \frac{4}{3} M^5\bar{P} \ \{\bar{u}(Q-\bar{u})\}^4}{(1-\bar{u})(\bar{u}-\bar{u}_s)(\bar{u}-\bar{u}_2)} \tag{11}$$

where

$$\bar{u}_2 = \frac{(\gamma-1)M^2+2}{(\gamma+1)M^2}, \quad \bar{u}_s = \frac{\gamma M^2+1}{(\gamma+1)M^2} \tag{12}$$

so that

$$1-\bar{u}_s = \bar{u}_s - \bar{u}_2. \tag{13}$$

Differential equation (11) has three singular points G_1, G_s, G_2 where

$$\left.\begin{aligned} G_1 &: \bar{u} = 1, \ \bar{h} = \bar{h}_1 \equiv \frac{4}{3} M^5\bar{P}(Q-1)^4 \\ G_i &: \bar{u} = \bar{u}_i, \ \bar{h} = \bar{h}_i \equiv \frac{4}{3} M^5\bar{P}\left\{\bar{u}_i(Q-\bar{u}_i)\right\}^4, \ i = 2, S \end{aligned}\right\} \tag{14}$$

G_1 is a saddle point and exactly two integral curves pass through this point, the slopes of the two integral curves at this point being

$$\overset{(1)}{\lambda_1}, \overset{(2)}{\lambda_1} = \frac{1}{2}\left\{\xi_1\eta_1 \pm (\xi_1^2\eta_1^2 + 4\xi_1)^{\frac{1}{2}}\right\} \tag{15}$$

where

$$\xi_1 = \frac{3(\gamma-1)^2 M^4}{(M^2-1)^2} > 0, \ \eta_1 = 4(\gamma M^2 - 1)\bar{h}_1 > 0 \tag{16}$$

so that

$$\overset{(1)}{\gamma_1} > 0, \ \overset{(2)}{\lambda_1} < 0.$$

Similarly G_2 is also a saddle point with exactly two integral curves passing through it with slopes

$$\overset{(1)}{\lambda_2}, \overset{(2)}{\lambda_2} = \frac{1}{2}\left\{\xi_1\eta_2 \pm (\xi_1^2\eta_2^2 + 4\xi_1)^{\frac{1}{2}}\right\} \tag{17}$$

where

$$\eta_2 = \frac{2(3-\gamma)\bar{h}_2}{\bar{u}_2}\left\{\frac{\frac{3\gamma-1}{\gamma(3-\gamma)} - M^2}{M^2 - \frac{\gamma-1}{2\gamma}}\right\}$$

and

$$\overset{(1)}{\lambda_2} > 0, \ \overset{(2)}{\lambda_2} < 0.$$

APPROXIMATE SOLUTION

We have seen from the phase plane analysis in reference 1 that the shock structure integral curve approaches the singular points G_1 and G_2 with negative slopes $\overset{(2)}{\lambda_1}$ and $\overset{(2)}{\lambda_2}$ respectively. Again if

$$\bar{P}^* = \frac{\sqrt{6}\,\gamma^4 (\gamma + 1)^7 \,|\, M^2 - 1 \,|\, M^7}{16 (\gamma - 1)^2 (\gamma M^2 + 1)^7}$$

then in the case $\bar{P} < \bar{P}^*$, an embedded shock appears in the shock structure and the portions of the integral curves which represent the front and the back of the shock are almost straight lines.

Assuming that in the front and at the back the velocity $\bar{u}$ is a linear function of $\bar{h}$, we have

$$\bar{u} = 1 + \overset{(2)}{\lambda_1} (\bar{h} - \bar{h}_1) \text{ for } \tau > 0 \tag{18}$$

and

$$\bar{u} = \bar{u}_2 + \overset{(2)}{\lambda_2} (\bar{h} - \bar{h}_2) \text{ for } \tau < 0. \tag{19}$$

If suffixes 3 and 4 to the flow variables refer to their values just ahead and just behind the embedded shock, then, since $\bar{F}$ and $\bar{h}$ are continuous across it, we have

$$\bar{F}_3 = \bar{F}_4 \equiv \bar{F}_e \quad (\text{say}) \tag{20}$$

and

$$\bar{h}_3 = \bar{h}_4 \equiv \bar{h}_e \quad (\text{say}) \tag{21}$$

From (9) and (20) we have

$$1 - \bar{u}_3 = \bar{u}_4 - \bar{u}_2 \tag{22}$$

From (18) and (19) the expressions for $\bar{u}_3$ and $\bar{u}_4$, when substituted in (22) give

$$\bar{h}_e = \frac{\overset{(2)}{\lambda_1} \bar{h}_1 + \overset{(2)}{\lambda_2} \bar{h}_2}{\overset{(2)}{\lambda_1} + \overset{(2)}{\lambda_2}}. \tag{23}$$

The jump in particle velocity across the embedded shock is given by

$$\bar{u}_3 - \bar{u}_4 = -2\lambda (\bar{h}_1 - \bar{h}_2) + (1 - \bar{u}_2) \tag{24}$$

Also, we have

$$\bar{F}_e = -\frac{(\gamma + 1)}{2(\gamma - 1)} \lambda \,.\, (\bar{h}_1 - \bar{h}_2) \Big[(1 - \bar{u}_2) - \lambda (\bar{h}_1 - \bar{h}_2) \Big] \tag{25}$$

$$\bar{u}_3 = 1 - \lambda (\bar{h}_1 - \bar{h}_2) \tag{26}$$

and

$$\bar{u}_4 = \bar{u}_2 + \lambda (\bar{h}_1 - \bar{h}_2) \tag{27}$$

where

$$\lambda = \frac{\overset{(1)}{\lambda_1}\ \overset{(2)}{\lambda_2}}{\overset{(2)}{\lambda_1} + \overset{(2)}{\lambda_2}}.$$

To determine the flow variables in terms of the optical thickness from the shock, we substitute $\bar{u}$ from (18) and (19) in (9) so that

$$\frac{d\bar{h}}{d\tau} = -\frac{(\gamma+1)}{2(\gamma-1)}\left\{\overset{(2)}{\lambda_1}\right\}^2 (\bar{h} - \bar{h}_1)\,(\bar{h}^{(1)} - \bar{h}), \text{ for } \tau > 0, \tag{28}$$

and

$$\frac{d\bar{h}}{d\tau} = -\frac{(\gamma+1)}{2(\gamma-1)}\left\{\overset{(2)}{\lambda_2}\right\}^2 \left(\bar{h} - \bar{h}^{(2)}\right)(\bar{h}_2 - \bar{h}); \text{ for } \tau < 0 \tag{29}$$

where

$$\bar{h}^{(1)} = \bar{h}_1 - \frac{1-\bar{u}_2}{\overset{(2)}{\lambda_1}} > \bar{h}_1 \tag{30}$$

and

$$\bar{h}^{(2)} = \bar{h}_2 + \frac{1-\bar{u}_2}{\overset{(2)}{\lambda_2}} < \bar{h}_2. \tag{31}$$

The solutions of equations (28) and (29) with the condition

$$\bar{h} = \bar{h}_e \quad \text{at} \quad \tau = 0$$

are

$$\bar{h} = \frac{\bar{h}_1 + \bar{h}^{(1)} f_1(\tau)}{1 + f_1(\tau)}, \quad \text{for } \tau > 0 \tag{32}$$

and

$$\bar{h} = \frac{\bar{h}^{(2)} + \bar{h}_2 f_2(\tau)}{1 + f_2(\tau)}, \quad \text{for } \tau < 0 \tag{33}$$

where

$$f_1(\tau) = \frac{\bar{h}_e - \bar{h}_1}{\bar{h}^{(1)} - \bar{h}_e} \exp\left[\frac{(\gamma+1)}{2(\gamma-1)}(1-\bar{u}_2)\,\overset{(2)}{\lambda_1}\,\tau\right] \tag{34}$$

and

$$f_2(\tau) = \frac{\bar{h}_e - \overset{(2)}{\bar{h}_2}}{\bar{h}_2 - \bar{h}_e} \exp\left[\frac{(\gamma+1)}{2(\gamma-1)}(1-\bar{u}_2)\,\overset{(2)}{\lambda_1}\,\tau\right]. \tag{35}$$

Thus we have obtained complete solution of the problem (32) and (33) give $\bar{h}$ in terms of τ, (18) and (19) give $\bar{u}$, (8) gives $\bar{p}_Q$, (9) gives $\bar{F}$ and finally

$$\bar{T} = \bar{u}\,(Q - \bar{u}) \tag{36}$$

gives the non-dimensional temperature.

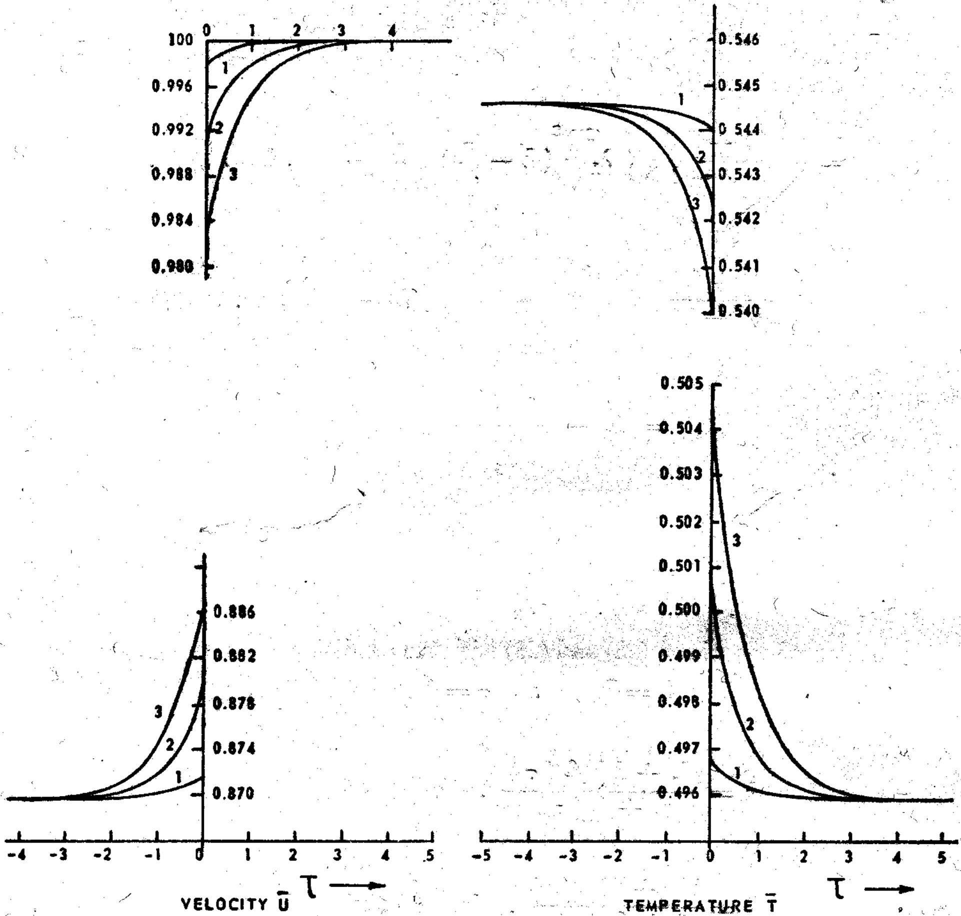

Fig. 1—Shock Structure in RGD [$1 : \bar{P} = 0{\cdot}01$; $2 : \bar{P} = 0{\cdot}05$; $3 : \bar{P} = 0{\cdot}1$]

RESULTS AND DISCUSSION

The numerical work has been done for the following six sets of values of M and $\bar{p}$ with $\gamma = 5/3$ and mean molecular weight $\frac{1}{2}$ as in the case of fully ionised hydrogen gas.

Table 1 gives the values of various flow variables at $\tau = +\infty$, $\tau = -\infty$ and at the embedded shock. Figs. 1-4 give the variation of various flow variables with the optical thickness from the shock. The values of $\bar{p}^*$ for $M = 1{\cdot}1$ and $1{\cdot}8$ (both $< M^*$) are $0{\cdot}46$ and $0{\cdot}80$ and we find from the general theory[1] that the shock structure should contain an embedded shock in each of the six cases except the last one where $M = 1{\cdot}8$ and $\bar{P} = 1$. However, the last case was taken in order to estimate the error in the present solution, which will show maximum error in this case. We find here that instead of getting a continuous profile, an embedded shock appears in between but the jumps in flow variable across it are very small.

TABLE 1

VARIOUS FLOW VARIABLES AT $\tau = \pm\infty$ AND AT THE EMBEDDED SHOCK

No.	1	2	3	4	5	6
M	1·1	1·1	1·1	1·8	1·8	1·8
$\bar{P}$	0·01	0·05	0·10	0·10	0·50	1.00
Q	1·4959	1·4959	1·4959	1·1852	1·1852	1·1852
$\bar{u}_1$	1	1	1	1	1	1
$\bar{u}_3$	0·9981	0·9909	0·9830	0·9744	0·8699	0·7519
$\bar{u}_s$	0·93492	0·93492	0·93492	0·74074	0·74074	0.74074
$\bar{u}_4$	0·8718	0·8790	0·8868	0·5071	0·6115	0·7296
$\bar{u}_2$	0·86983	0·86983	0·86983	0·48148	0·48148	0·48148
$\bar{h}_1$	$1{\cdot}298\times10^{-3}$	$6{\cdot}491\times10^{-3}$	$1{\cdot}298\times10^{-2}$	$2{\cdot}963\times10^{-3}$	$1{\cdot}481\times10^{-2}$	$2{\cdot}963\times10^{-2}$
$\bar{h}_e$	$1{\cdot}594\times10^{-3}$	$7{\cdot}990\times10^{-3}$	$1{\cdot}603\times10^{-2}$	$1{\cdot}896\times10^{-2}$	$1{\cdot}115\times10^{-1}$	$2{\cdot}564\times10^{-1}$
$\bar{h}_s$	$1{\cdot}624\times10^{-3}$	$8{\cdot}122\times10^{-3}$	$1{\cdot}624\times10^{-2}$	$2{\cdot}960\times10^{-2}$	$1{\cdot}480\times10^{-1}$	$2{\cdot}960\times10^{-1}$
$\bar{h}_2$	$1{\cdot}888\times10^{-3}$	$9{\cdot}441\times10^{-3}$	$1{\cdot}888\times10^{-2}$	$3{\cdot}320\times10^{-2}$	$1{\cdot}660\times10^{-1}$	$3{\cdot}320\times10^{-1}$
$\bar{p}_{G1}$	0·4959	0·4959	0·4959	0·1853	0·1853	0·1853
$\bar{p}_{G3}$	0·4978	0·5050	0·5129	0·2108	0·3153	0.4333
$\bar{p}_{G4}$	0·6241	0·6169	0·6090	0·6781	0·5736	0·4556
$\bar{p}_{G2}$	0·6260	0·6260	0·6260	0·7036	0·7036	0·7036
$\bar{T}_1$	0·4959	0·4959	0.4959	0·1852	0·1852	0·1852
$\bar{T}_3$	0·4968	0·5004	0·5041	0·2054	0·2742	0·3258
$\bar{T}_4$	0·5441	0·5422	0·5401	0·3438	0·3508	0·3324
$\bar{T}_2$	0·5446	0·5446	0·5446	0·3388	0·3388	0·3388
$\bar{F}_e$	$-4{\cdot}962\times10^{-4}$	$-2{\cdot}210\times10^{-3}$	$-3{\cdot}848\times10^{-3}$	$-2{\cdot}522\times10^{-2}$	$-1{\cdot}010\times10^{-1}$	$-1{\cdot}342\times10^{-1}$

We note the following facts from Figs. 1–4 :

(*i*) In all the three cases for the weak shock, the two uniform states 1 and 2 are attained at almost equal optical depths from the embedded shock. This is true even when $M = 1{\cdot}8$ with $\bar{P} = 0{\cdot}1$, i.e. when the radiation is weak. However, in the last two cases the flow variables attain their asymptotic values over an optical depth which is very small for the back as compared to that for the front of the shock.

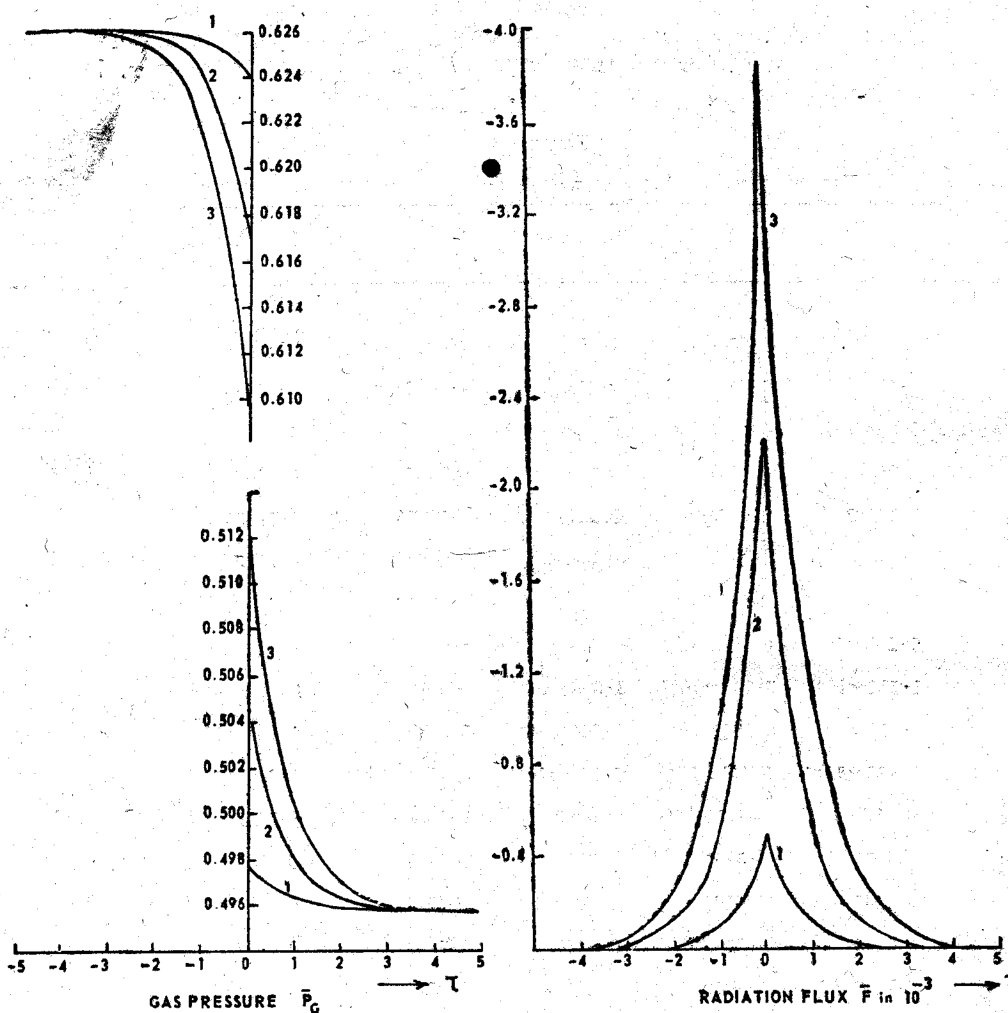

Fig. 2—Shock structure; in RGD [1 : $\bar{P}$ = 0·01; 2 : $\bar{P}$ = 0·05; 3 : $\bar{P}$ = 0·1]

(*ii*) In all the six cases $1 - \hat{u}_3 \simeq \hat{u}_4 - \hat{u}_2$, $\bar{p}_{G3} - \bar{p}_{G1} \simeq \bar{p}_{G2} - \bar{p}_{G4}$, i.e. the variations in velocity and pressure in the front and the back are almost equal. The change in temperature $\bar{T}_3 - \bar{T}_1$ in the front is more than the change $| \bar{T}_2 - \bar{T}_4 |$ in the back. The temperature is maximum at $\tau = -\infty$ in cases 1, 2, 3 and just behind the embedded shock in case 4, but in cases 5 and 6 the temperature is maximum not just behind the embedded shock but in the interior of the flow behind it.

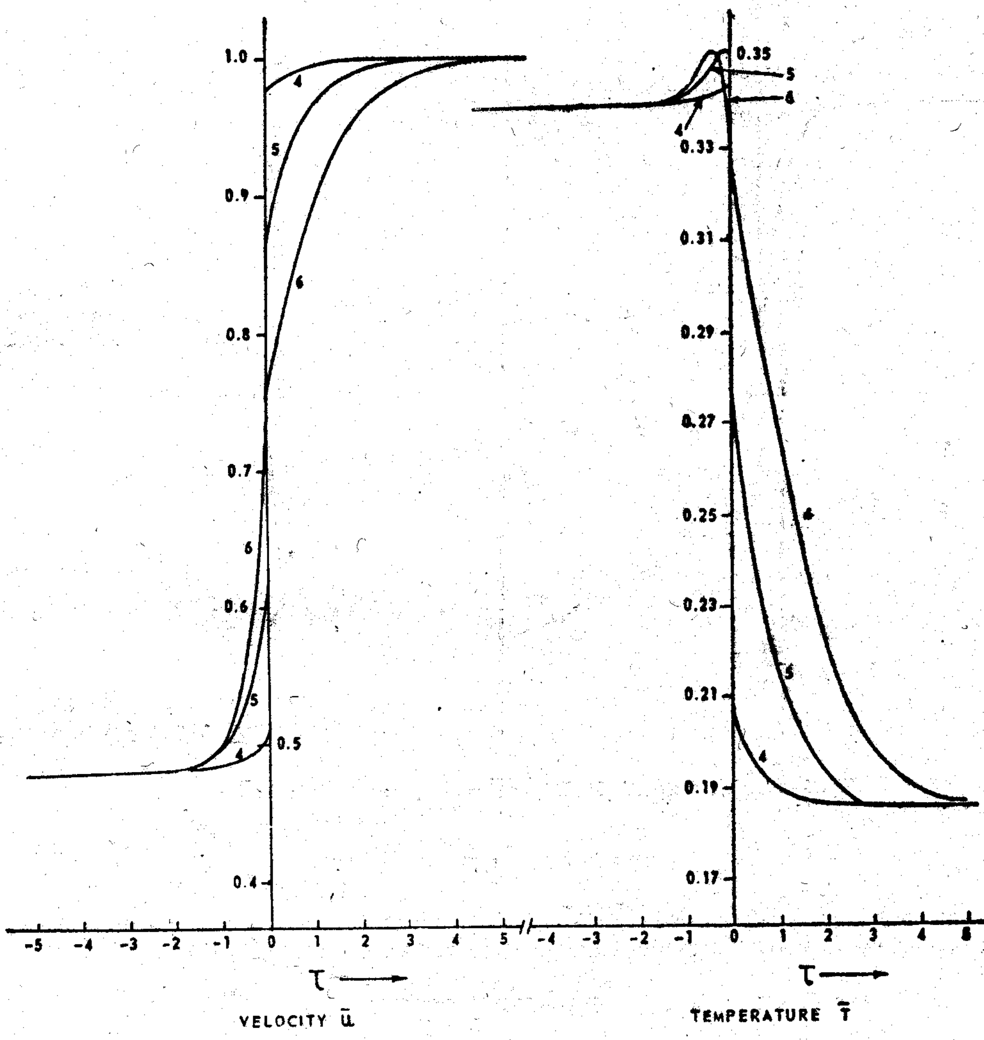

Fig. 3—Shock Structure in RGD [$4 : \bar{P} = 0 \cdot 1$; $5 : \bar{P} = 0 \cdot 5$; $6 : \bar{P} = 1 \cdot 0$]

(*iii*) The flux is symmetrical on the two sides with respect to the optical depth from the embedded shock in all the three cases with $M = 1 \cdot 1$ but this is not the case when $M = 1 \cdot 8$.

We finally remark that the analytical expressions for the flow variables in terms of optical thickness are so simple that they may prove useful for many other problems in RGD. We can also rely on the accuracy of the present solution when $\bar{P} << \bar{P}^*$ since we find that in case 2 the numerical results, presented here, cannot be distinguished on the graph from the graphical solution as presented in the Fig. 2 of Prasad[1].

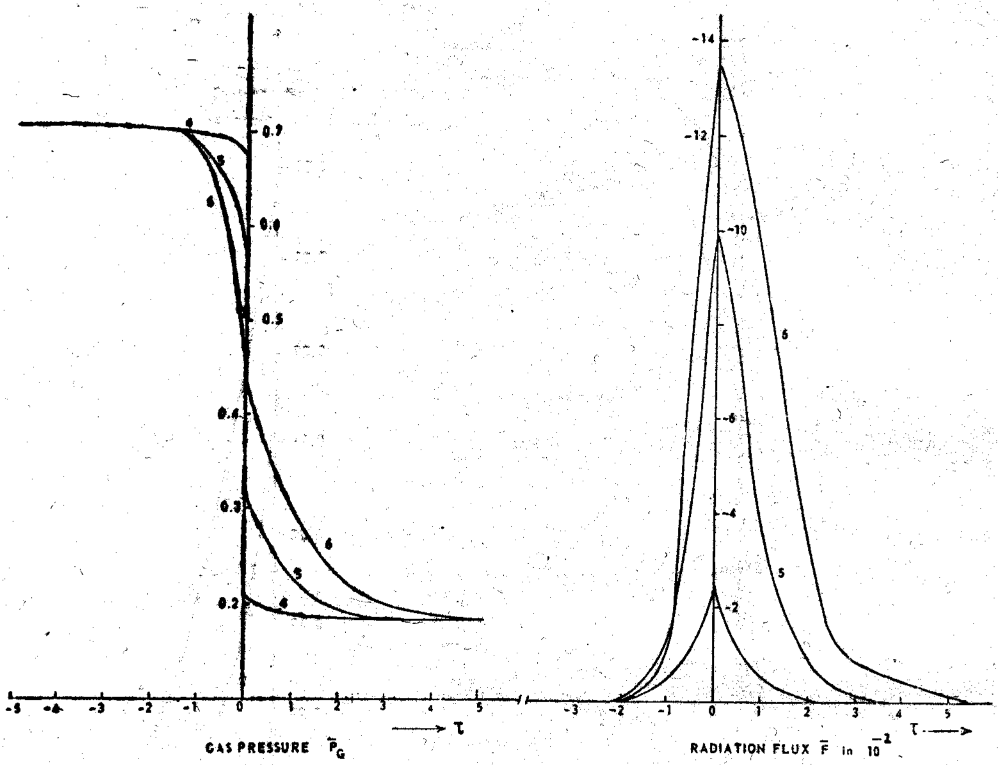

Fig. 4—Shock structure in RGD [4 : $\bar{P}$ = 0·1; 5 : $\bar{P}$ = 0·5; 6 : $\bar{P}$ = 1·0]

ACKNOWLEDGEMENT

The author expresses his deep sense of gratitude to Prof. P. L. Bhatnagar for help and encouragement throughout the preparation of this paper.

REFERENCES

1. PRASAD, P., "A Class of Steady State Flows and General Shock Structure Problem in RGD", *J. Mech. & Appl. Maths.* (in Press).

2. ZEL'DOVICH, I. B., *Soviet Physics*—JETP, 5 (1957), 919.

3. HEASLET, M. A. & BALDWIN, B. S., *Physics of Fluids*, 6 (1963), 781.

4. LICK, W., *Advances in Applied Mechanics*, 10, Fascicle 1.

5. VINCENTI, W. G. & KRUGER, C. H., "Introduction to Physical Gas-Dynamics" (John Wiley and Sons Inc., New York), 1965.